



Investigation on threshold voltage of p-channel GaN MOSFETs based on p-GaN/AlGaIn/GaN heterostructure

Ruo-Han Li(李若晗), Wu-Xiong Fei(费武雄), Rui Tang(唐锐), Zhao-Xi Wu(吴照玺), Chao Duan(段超), Tao Zhang(张涛), Dan Zhu(朱丹), Wei-Hang Zhang(张苇杭), Sheng-Lei Zhao(赵胜雷), Jin-Cheng Zhang(张进成), and Yue Hao(郝跃)

Citation: Chin. Phys. B, 2021, 30 (8): 087305. DOI: 10.1088/1674-1056/ac0793

Journal homepage: <http://cpb.iphy.ac.cn>; <http://iopscience.iop.org/cpb>

What follows is a list of articles you may be interested in

Investigation on threshold voltage of p-channel GaN MOSFETs based on p-GaN/AlGaIn/GaN heterostructure

Ruo-Han Li(李若晗), Wu-Xiong Fei(费武雄), Rui Tang(唐锐), Zhao-Xi Wu(吴照玺), Chao Duan(段超), Tao Zhang(张涛), Dan Zhu(朱丹), Wei-Hang Zhang(张苇杭), Sheng-Lei Zhao(赵胜雷), Jin-Cheng Zhang(张进成), and Yue Hao(郝跃)

Chin. Phys. B, 2021, 30 (8): 087305. DOI: 10.1088/1674-1056/ac0793

Ferroelectric effect and equivalent polarization charge model of $\text{PbZr}_{0.2}\text{Ti}_{0.8}\text{O}_3$ on AlGaIn/GaN MIS-HEMT

Yao-Peng Zhao(赵焱澎), Chong Wang(王冲), Xue-Feng Zheng(郑雪峰), Xiao-Hua Ma(马晓华), Ang Li(李昂), Kai Liu(刘凯), Yun-Long He(何云龙), Xiao-Li Lu(陆小力) and Yue Hao(郝跃)

Chin. Phys. B, 2021, 30 (5): 057302. DOI: 10.1088/1674-1056/abd469

Comparative study on characteristics of Si-based AlGaIn/GaN recessed MIS-HEMTs with HfO_2 and Al_2O_3 gate insulators

Yao-Peng Zhao(赵焱澎), Chong Wang(王冲), Xue-Feng Zheng(郑雪峰), Xiao-Hua Ma(马晓华), Kai Liu(刘凯), Ang Li(李昂), Yun-Long He(何云龙), Yue Hao(郝跃)

Chin. Phys. B, 2020, 29 (8): 087304. DOI: 10.1088/1674-1056/ab8daa

Negative bias-induced threshold voltage instability and zener/interface trapping mechanism in GaN-based MIS-HEMTs

Qing Zhu(朱青), Xiao-Hua Ma(马晓华), Yi-Lin Chen(陈怡霖), Bin Hou(侯斌), Jie-Jie Zhu(祝杰杰), Meng Zhang(张濛), Mei Wu(武玫), Ling Yang(杨凌), Yue Hao(郝跃)

Chin. Phys. B, 2020, 29 (4): 047304. DOI: 10.1088/1674-1056/ab7809

Non-recessed-gate quasi-E-mode double heterojunction AlGaIn/GaN high electron mobility transistor with high breakdown voltage

Mi Min-Han, Zhang Kai, Chen Xing, Zhao Sheng-Lei, Wang Chong, Zhang Jin-Cheng, Ma Xiao-Hua, Hao Yue

Chin. Phys. B, 2014, 23 (7): 077304. DOI: 10.1088/1674-1056/23/7/077304

Investigation on threshold voltage of p-channel GaN MOSFETs based on p-GaN/AlGaIn/GaN heterostructure*

Ruo-Han Li(李若晗)¹, Wu-Xiong Fei(费武雄)², Rui Tang(唐锐)², Zhao-Xi Wu(吴照玺)³,
Chao Duan(段超)³, Tao Zhang(张涛)¹, Dan Zhu(朱丹)¹, Wei-Hang Zhang(张苇杭)¹,
Sheng-Lei Zhao(赵胜雷)^{1,†}, Jin-Cheng Zhang(张进成)^{1,‡}, and Yue Hao(郝跃)¹

¹Key Laboratory of Wide Band-Gap Semiconductors and Devices, School of Microelectronics,
Xidian University, Xi'an 710071, China

²China Electronic Product Reliability and Environmental Testing Research Institute, Guangzhou 510610, China

³China Aerospace Components Engineering Center, Beijing 100094, China

(Received 2 March 2021; revised manuscript received 13 May 2021; accepted manuscript online 3 June 2021)

The threshold voltage (V_{th}) of the p-channel metal–oxide–semiconductor field-effect transistors (MOSFETs) is investigated via Silvaco-Atlas simulations. The main factors which influence the threshold voltage of p-channel GaN MOSFETs are barrier height $\Phi_{1,p}$, polarization charge density σ_b , and equivalent unit capacitance C_{oc} . It is found that the thinner thickness of p-GaN layer and oxide layer will acquire the more negative threshold voltage V_{th} , and threshold voltage $|V_{th}|$ increases with the reduction in p-GaN doping concentration and the work-function of gate metal. Meanwhile, the increase in gate dielectric relative permittivity may cause the increase in threshold voltage $|V_{th}|$. Additionally, the parameter influencing output current most is the p-GaN doping concentration, and the maximum current density is 9.5 mA/mm with p-type doping concentration of $9.5 \times 10^{16} \text{ cm}^{-3}$ at $V_{GS} = -12 \text{ V}$ and $V_{DS} = -10 \text{ V}$.

Keywords: p-channel GaN MOSFETs, enhancement mode (E-mode), threshold voltage

PACS: 73.40.Kp, 73.61.Ey, 78.30.Fs

DOI: 10.1088/1674-1056/ac0793

1. Introduction

N-type GaN transistors have been concerned widely and developed rapidly due to the superior performance for power switching.^[1] However, p-channel devices have attracted less attention than n-channel counterparts for the low mobility of holes (*i.e.*, the reported maximum value is about $24 \text{ cm}^2/(\text{V}\cdot\text{s})$ ^[2]) which leads to poor current characteristics and switching speed, and the performance of complementary metal–oxide–semiconductor (CMOS) is limited by p-channel MOSFETs. In order to enhance the characteristic of hole-based devices, two-dimensional hole gas (2DHG) is indeed needed for breaking through the limitation. Various authors have come up with the prototypes about polarization heterostructure inducing hole gas, like GaN/AlGaIn/GaN polarization superjunction device,^[3] GaN/AlIn p-channel transistor,^[4] and the advanced GaN CMOS technology.^[5] Simultaneously, Akira Nakajima *et al.*^[6] have demonstrated the methods to increase the concentration of 2DHG. So far, an E-mode GaN-based p-channel MOSFET with a negative threshold voltage of -2.7 V is integrated with an n-channel counterpart.^[7] Nadim Chowdhury *et al.*^[8] have demonstrated a p-GaN/AlGaIn/GaN MOSFET exhibiting a low on-resistance (R_{ON}) of $\sim 2.3 \text{ k}\Omega\cdot\text{mm}$ and an

output current of 1.1 mA/mm at $V_{DS} = -5 \text{ V}$ and $V_{GS} = -11 \text{ V}$. Zheng *et al.*^[9] have investigated the device with a higher output current of 6.1 mA/mm at $V_{DS} = -10 \text{ V}$ and $V_{GS} = -12 \text{ V}$, a high ON/OFF ratio of $\sim 10^7$, and a negative threshold voltage of -1.7 V . The formation of 2DHG is similar to that of 2DEG. The strong piezoelectric and spontaneous polarization effect exists between the GaN/AlGaIn interface, which results to the accumulation of negative polarization charges,^[10] and 2DHG is obtained over it.

With the development of GaN-based power transistors, the application of p-channel GaN devices is expected to further exploit, such as single-stage GaN complementary logic inverters and monolithic integration of GaN-based complementary circuits for driving, sensing, and control. Although p-channel GaN devices are not perfect candidates for high-speed circuits, the advantages including reducing the inductance, achieving larger wafer size, and having less operating speed are needed for circuit design. As an important component in CMOS, p-channel GaN/AlGaIn/GaN MOSFETs deliver hole current through 2DHG induced by polarization effect, so the devices are intrinsically normally-on. However, normally-off p-channel GaN transistors with high threshold voltage and low leakage current highly improve the performance of circuits. As for the great advantages of the enhancement mode (E-

*Project supported by the Key-Area Research and Development Program of Guangdong Province, China (Grant Nos. 2020B010174001 and 2020B010171002), the Ningbo Science and Technology Innovation Program 2025 (Grant No. 2019B10123), and the National Natural Science Foundation of China (Grant No. 62074122).

†Corresponding author. E-mail: slzhao@xidian.edu.cn

‡Corresponding author. E-mail: jchzhang@xidian.edu.cn

mode) MOSFETs compared to the depletion mode (D-mode) MOSFETs in power switching application,^[11] several measures are proposed to make E-mode operation achieved, such as gate recessing, ion implantation, or polarization engineering. It is necessary to carry out the investigation on the factors affecting threshold voltage of the E-mode p-channel MOSFETs.

In this work, the effects of the key parameters on threshold voltage of E-mode p-GaN MOSFET were investigated, such as the thickness of p-GaN under the gate L_p , the doping concentration of p-GaN N_p , the thickness of gate dielectric t_{ox} , the dielectric relative permittivity of gate dielectric γ , and the work-function of gate metal W_m . And then, output current can be risen simultaneously by optimizing the parameters. According to the simulation results, the maximum output current ($-I_D$) is about 9.5 mA/mm at $V_{GS} = -12$ V and $V_{DS} = -10$ V. All the simulations are performed in Silvaco-Atlas simulation software.

2. Device structure

Figure 1 depicts the cross-sectional view of p-channel GaN MOSFETs, which includes recessed gate and p-GaN/AlGaIn/GaN double heterostructure. The structure of this device consists of a 4.5- μm n-GaN buffer layer, a 12-nm $\text{Al}_{0.2}\text{Ga}_{0.8}\text{N}$ barrier layer, an 85-nm p-GaN channel layer with

the doping concentration of $6.5 \times 10^{16} \text{ cm}^{-3}$, and gated oxide layer from bottom to top. The 2DEG and 2DHG are induced by the strain of lattice mismatch between AlGaIn/n-GaN and p-GaN/AlGaIn, respectively. Al_2O_3 is utilized to form gated oxide layer on the top of p-GaN layer to suppress the gate leakage current. SiO_2 is introduced to define the length and width of Al_2O_3 around the side of the gate. Additional, recessed gate makes E-mode operation achieved. The gate region is formed with Ni whose work-function is 5.2 eV. Besides, both of the source region and the drain region are ohmic contacts to the p-GaN channel layer, in which the doping concentration of p type is set to $2.0 \times 10^{18} \text{ cm}^{-3}$. More details about structural and physical parameters are listed in Table 1.

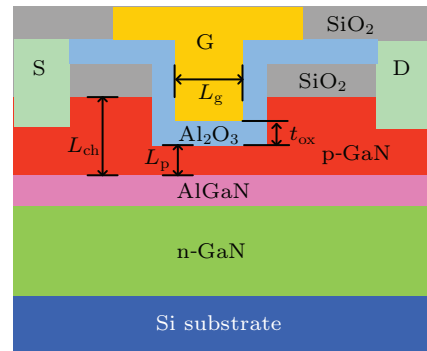


Fig. 1. Cross-section of the recessed-gate E-mode p-GaN/AlGaIn/GaN MOSFET.

Table 1. Key structural and physical parameters of p-channel GaN MOSFET.

Parameters	Unit	Values	Description
L_{ch}	nm	85	p-GaN layer thickness
L_p	nm	31	p-GaN layer thicknesses under the gate
N_p	cm^{-3}	6.5×10^{16} (p type)	p-GaN layer doping concentration
L_{bar}	nm	12	AlGaIn barrier thickness
N_{AlGaIn}	cm^{-3}	3×10^{14} (n type)	AlGaIn barrier doping concentration
σ_h	cm^{-2}	6.5×10^{12}	2DHG density
t_{ox}	nm	20	gate dielectric thicknesses
W_m	eV	5.2	gate metal work function
L_g	μm	4	Gate length
L_{gs}	μm	2	distance between gate and source
L_{gd}	μm	4	distance between gate and drain

The energy band diagrams for the oxide/p-GaN/AlGaIn/GaN displayed in Fig. 2, in which the features of conduction band and valence band are clearly presented. When the thickness of p-GaN layer is 85 nm as shown in Fig. 2(a), 2DHG and 2DEG are easily obvious in the interface of p-GaN/AlGaIn and AlGaIn/GaN, respectively. The structure with thinner p-GaN layer causes a shaper band bending, which prevents the intersection of valence band and Fermi energy at p-GaN/AlGaIn heterointerface (Fig. 2(b)), thus E-mode behavior is achieved.

The hole mobility under the recessed gate is defined at $10 \text{ cm}^2/\text{V} \cdot \text{s}$ in order to simulate the material damage caused by the etching process. And the limiting effect of electronic

traps should be concerned because of the distribution of quasi-static charge. According to the analysis of trapping effects in GaN material,^[12] the energy level of 2.85 eV and 1.75 eV below the conduction band ($E_C - 2.85 \text{ eV}$ and $E_C - 1.75 \text{ eV}$) are the important energy levels related to current collapse. In this simulation, $E_C - 2.85 \text{ eV}$ and $E_C - 2.9 \text{ eV}$ are set as a deep acceptor level (E_{DA}) and a deep donor level (E_{DD}), respectively. Other parameters completing the trap model are listed in Table 2. Besides trap model, field-dependent mobility (FLDMOB) model, Shockley–Read–Hall (SRH) recombination model, and Fermi–Dirac statistics are also considered in our simulation. The simulation parameters of p-channel GaN MOSFET are calibrated with the reported experimental

result.^[9] Therefore, the simulating results of transfer and output characteristics are similar to that of reported experiment, shown in Fig. 3.

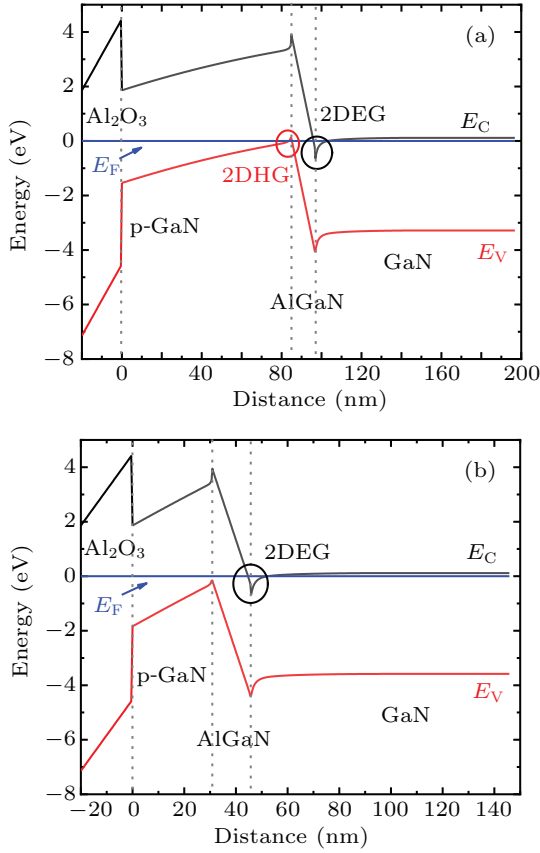


Fig. 2. The simulated band diagrams of a structure with an oxide/p-GaN/AlGaIn/GaN. It is clearly visible that the thickness of p-GaN in panels (a) and (b) are 85 nm and 31 nm, respectively.

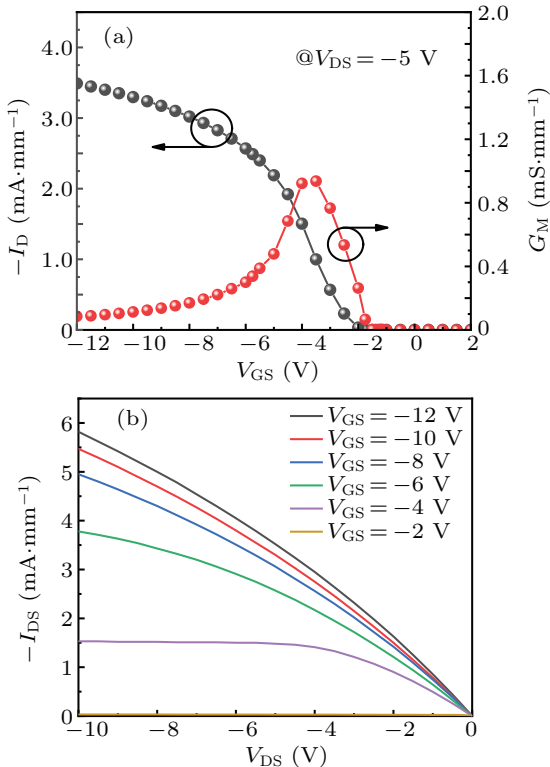


Fig. 3. (a) Transfer and (b) output characteristics of the E-mode p-GaN-MOSFET. The doping concentration of p-GaN is set as $6.5 \times 10^{16} \text{ cm}^{-3}$.

Table 2. The parameters of trap model in this p-channel GaN.

Parameters	Unit	Values
e.level (donor/acceptor)	eV	2.9/2.85
Density (donor/acceptor)	cm^{-3}	$8.0 \times 10^{16}/6.5 \times 10^{16}$
Sign (donor/acceptor)	cm^2	$5 \times 10^{-15}/5 \times 10^{-13}$
Sigp	cm^2	1×10^{-15}
Degen	/	1

3. Results and discussion

The model analysis and theoretical calculation to the typical double heterostructure with 2DHG and 2DEG have been prepared to obtain an effective high threshold voltage $|V_{th}|$ in the p-channel structure. According to Poisson equations, carrier continuity, and Gauss laws, the function of 2DHG density at interface and threshold voltage can be defined, and then the factors influencing threshold voltage can be explained mathematically. According to the model put forward by Ashwani Kumar,^[13] the threshold voltage can be expressed as

$$V_{th} = \frac{\sigma_b}{C_{oc}} - \frac{C_b}{C_{oc}} \frac{E_G}{e} - \frac{\sigma_{ox}}{C_{ox}} - \frac{\Phi_{1,p}}{e} + \frac{\Delta E_{OV}}{e}, \quad (1)$$

where $\Phi_{1,p}$ is the barrier height of the valence band at gate/oxide interface, ΔE_{OV} is the valence band offset between the oxide and GaN channel, σ_{ox} is the net sheet charge density at oxide/GaN interface and σ_b is the net polarization sheet charge density at GaN/AlGaIn interface. C_b and C_{ox} are unit area capacitance in AlGaIn layer and oxide, respectively. And C_{oc} is the equivalent unit capacitance offered by the oxide and channel layers, which is defined by $C_{oc} = (1/C_{ox} + 1/C_{ch})^{-1}$. From expression (1), what it comes down to is that there are three parameters influencing V_{th} most, namely, barrier height $\Phi_{1,p}$, polarization charge density σ_b , and equivalent unit capacitance C_{oc} .

The threshold voltage engineering can be performed by changing these three parameters, such as p-GaN layer thickness, work-function of gate metal, oxide thickness, and so on. The results of investigation on threshold voltage of p-channel GaN MOSFETs will be described below in detail.

In this section, the impact on the threshold voltage of five major parameters (L_p , N_p , t_{ox} , γ , and W_m) is discussed. In principle, band diagrams and analytic calculation model can distinctly emphasize the features, which are helpful to understand the changes of threshold voltage. Figure 4(a) shows the transfer characteristic of the E-mode p-GaN MOSFETs shifts with various doping concentrations of the p-GaN layer. It is worth noting that variable parameter is the only one, under the premise of other parameters remaining constant. Specific values and structures follow Table 1 and Fig. 1. While the doping concentration N_p decreases from $9.5 \times 10^{16} \text{ cm}^{-3}$ to $4.0 \times 10^{16} \text{ cm}^{-3}$, the threshold voltage $|V_{th}|$ increases from 1.5 V to 2.25 V as well as the source current ($-I_D$) drops from 5.7 mA/mm to 1.6 mA/mm. The shift of $|V_{th}|$ and $-I_D$ can be explained by comparing the conduction band diagram of

p-GaN/AlGaN/GaN structure at different p-GaN doping concentrations. As shown in Fig. 4(b), the conduction band of the p-GaN/AlGaN/GaN with a high doping concentration makes conduction band beyond the Fermi energy and valence band near the Fermi energy at the same time, which makes V_{th} shift to be positive.

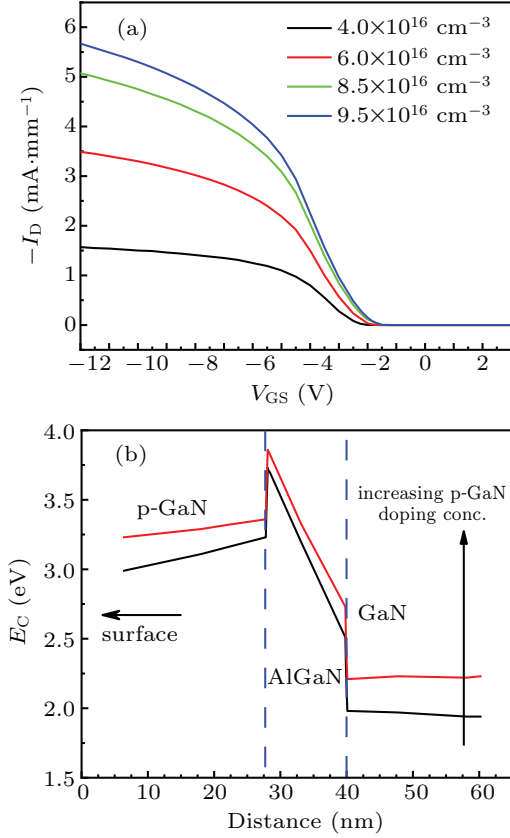


Fig. 4. Transfer characteristics of the E-mode p-GaN-MOSFET with various N_p from $4.0 \times 10^{16} \text{ cm}^{-3}$ to $9.5 \times 10^{16} \text{ cm}^{-3}$. (b) The simulating band diagram of p-GaN/AlGaN/GaN structure.

When the thickness of the p-GaN layer under the gate L_p varies from 35 nm to 10 nm, the threshold voltage $|V_{th}|$ shifts from 1.5 V to 2.5 V. And the source current ($-I_D$) decreases from 4.2 mA/mm to 2.2 mA/mm as shown in Fig. 5(a). While the thickness of Al_2O_3 t_{ox} varies from 30 nm to 10 nm, the threshold voltage $|V_{th}|$ increases, from 1.75 V to 2.25 V with negligible change of source current ($-I_D$) as depicted in Fig. 5(b). From the perspective of the energy band, thinner p-GaN channel layer and Al_2O_3 thickness make the energy band bend more sharply in their layers, which makes the valence band at the interface of p-GaN/AlGaN lower than the Fermi energy and the V_{th} is more negative. It is obvious that the thickness of p-GaN layer L_p has a significantly greater effect on the threshold voltage V_{th} than the thickness of Al_2O_3 layer t_{ox} from Figs. 5(a) and 5(b).

In addition, the threshold voltage $|V_{th}|$ would increase not only because of the reduction in gate dielectric thickness, but because the gate dielectric relative permittivity increases. According to the direct proportion of oxide capacitance and permittivity, which can be expressed as $C_{ox} \propto \gamma_{ox} \gamma_0 / t_{ox}$. The rise

in permittivity γ_{ox} will cause an increase in capacitance C_{ox} with a constant value of the thickness of oxide layer t_{ox} . Meanwhile, the ionized impurities in p-GaN layer are constant when the doping concentration in p-GaN layer N_p remains a certain value. Therefore, the positive charge density generated under the gate Q_s keeps a constant, too. According to the equation $V_{oxide} = Q_s / C_{ox}$, the voltage added to oxide layer V_{oxide} drops followed by the increase in C_{ox} . The results are that energy band bends gentle and valence band reaches a lower level. Thus, the higher C_{ox} makes the threshold voltage V_{th} more negative. Figure 6(a) presents the transfer characteristic of these devices with different gate dielectrics, which reflects the relationship between gate dielectric relative permittivities γ and threshold voltage V_{th} . Three kinds of gate dielectrics, such as SiO_2 , Al_2O_3 , and HfO_2 , with various permittivities γ of 3.9, 9.0, and 25.0, respectively, are considered in our simulation. When the permittivities γ changes from 3.9 to 25, the threshold voltage $|V_{th}|$ offsets from 1.5 V to 2.25 V, and the source current ($-I_D$) increases from 3.3 mA/mm to 3.7 mA/mm.

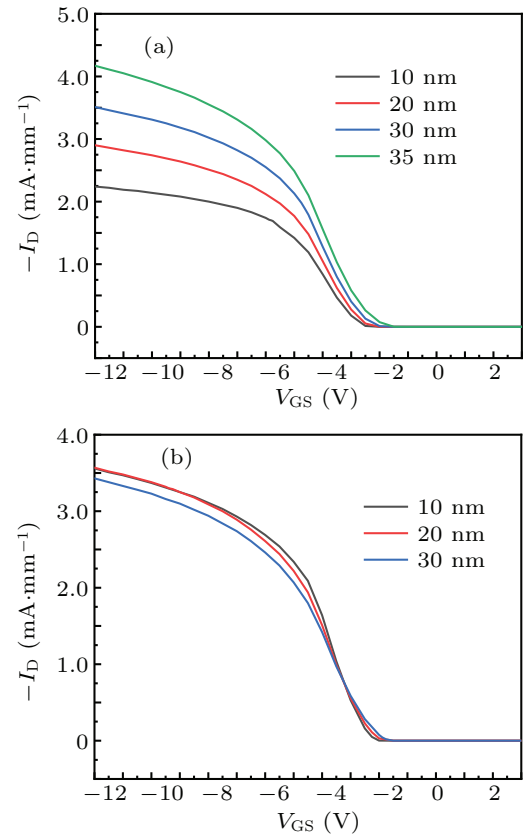


Fig. 5. Transfer characteristics of the E-mode p-GaN-MOSFET with various (a) p-GaN layer thicknesses under the gate and (b) Al_2O_3 thicknesses under the gate.

Figure 6(b) shows the effect of gate metal work-function on the threshold voltage V_{th} . The barrier height is directly affected by the work-function, from Eq. (1). Because of the p-type Schottky barrier, the reduction in gate metal work function W_m can lead to the increase in barrier height $\phi_{1,p}$, driving the device towards an E-mode regime. While the work-function of gate metal drops from 6.0 to 4.2 in the threshold

voltage $|V_{th}|$ shows a significantly increase from 1 V to 3 V, and the source current ($-I_D$) shows negligible change from the simulation, which means that the work-function of gate metal shows no effect on the source current of the device.

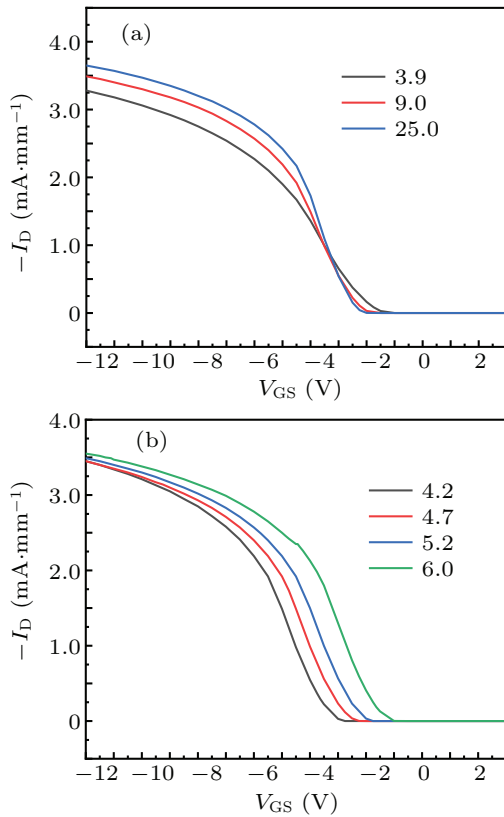


Fig. 6. Transfer characteristics of the E-mode p-GaN-MOSFET with various (a) gate dielectric relative permittivities and (b) gate metal work-functions.

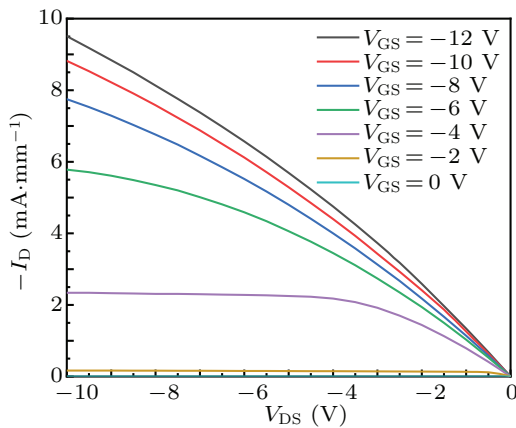


Fig. 7. Output characteristics of the E-mode p-GaN-MOSFET. The doping concentration of p-GaN is set as $9.5 \times 10^{16} \text{ cm}^{-3}$.

This simulation has taken effective measures to change the threshold voltage. Comparing the source current ($-I_D$) in transfer curves (Figs. 4(a), 5(a), 5(b), 6(a), and 6(b)), the most obvious way to boost current density is increasing the doping concentration of p-GaN N_p . Figure 7 presents the output characteristics under the condition of N_p of $9.5 \times 10^{16} \text{ cm}^{-3}$,

which shows the maximum current density of 9.5 mA/mm at $V_{GS} = -12 \text{ V}$ and $V_{DS} = -10 \text{ V}$.

4. Conclusion

In this paper, an E-mode p-channel GaN MOSFET is investigated by Silvaco-Atlas, in which 2DHG is induced by negative polarization charges at the interface of p-GaN/AlGaIn. Based on the theoretical analysis, the investigation on threshold voltage of p-channel GaN MOSFETs in p-GaN/AlGaIn/GaN heterostructure is carried out. It is found that the structural parameters of the devices have an obvious impact on threshold voltage. First, the threshold voltage $|V_{th}|$ increases from 1.5 V to 2.5 V with the decrease in p-GaN layer thicknesses under the gate L_p from 35 nm to 10 nm. And gate dielectric (Al_2O_3) thicknesses t_{ox} shows the same effect on threshold voltage as L_p . Meanwhile, the reduction in p-GaN layer doping concentrations N_p from $9.5 \times 10^{16} \text{ cm}^{-3}$ to $4.0 \times 10^{16} \text{ cm}^{-3}$ will make an increase in threshold voltage $|V_{th}|$ from 1.5 V to 2.25 V. Besides, threshold voltage $|V_{th}|$ may rise from 1.5 V to 2.25 V with the increase in gate dielectric relative permittivities γ from 3.9 to 25. In addition, the decrease in gate metal work functions W_m from 6.0 to 4.2 results the boost in $|V_{th}|$ from 1 V to 3 V. Finally, the output curve indicates that the maximum current density is about 9.5 mA/mm at $V_{DS} = -10 \text{ V}$ and $V_{GS} = -12 \text{ V}$ in this device. These simulated results offer more understanding of threshold voltage engineering of p-channel GaN MOSFETs.

References

- [1] Wu Y F, Gritters J, Shen L, Smith R P and Swenson B 2014 *IEEE Trans. Power Electron.* **29** 2634
- [2] Smorchkova I P, Haus E, Heying B, Kozodoy P, Fini P, Ibbetson J P, Keller S, DenBaars S P, Speck J S and Mishra U K 2000 *Appl. Phys. Lett.* **76** 718
- [3] Nakajima A, Sumida Y, Dhyani M H, Kawai H and Narayanan E M 2011 *IEEE Electron Dev. Lett.* **32** 542
- [4] Li G W, Wang R H, Song B, Verma J, Cao Y, Ganguly S, Verma A, Guo J, Xing H G and Jena D 2013 *IEEE Electron Dev. Lett.* **34** 852
- [5] Chu R M, Cao Y, Chen M, Li R and Zehnder D 2016 *IEEE Electron Dev. Lett.* **37** 269
- [6] Nakajima A, Sumida Y, Dhyani M H, Kawai H and Narayanan E M S 2010 *Appl. Phys. Express* **3** 121004
- [7] Nakajima A, Kubota S, Tsutsui K, Kakushima K, Wakabayashi H, Iwai H, Nishizawa S and Ohashi H 2017 *IET Power Electron* **11** 689
- [8] Chowdhury N, Lemettinen J, Xie Q Y, Zhang Y H, Rajput N S, Xiang P, Cheng K, Suihkonen S, Then H W and Palacios T 2019 *IEEE Electron Dev. Lett.* **40** 103
- [9] Zheng Z Y, Song W J, Zhang L, Yang S, Wei J and Chen K J 2020 *IEEE Electron Dev. Lett.* **41** 26
- [10] Hackenbuchner S, Majewski J A, Zandler G and Vogl P 2001 *J. Cryst. Growth* **230** 607
- [11] Motorola. (U.S. Patent) 3683 202 [1972-08-08]
- [12] Binari S C, Klein P B and Kazior T E. 2002 *Proc. IEEE* **90** 1048
- [13] Kumar A and Souza M M D 2018 *IET Power Electron* **11** 675